Dual epitope targeting and enhanced hexamerization by DR5 antibodies as a novel approach to induce potent antitumor activity through DR5 agonism

Overdijk, M.B.; Strumane, K.; Beurskens, F.J.; Buijsse, A.O.; Vermot-Desroches, C.; Vuillermoz, B.S.; ... ; Breij, E.C.W.

Dual Epitope Targeting and Enhanced Hexamerization by DR5 Antibodies as a Novel Approach to Induce Potent Antitumor Activity Through DR5 Agonism

Marije B. Overdijk[1], Kristin Strumane[1], Frank J. Beurskens[1], Antonio Ortiz Buijsse[1], Claudine Vermot-Desroches[2], Boris S. Vuillermoz[2], Thessa Kroes[1], Bart de Jong[1], Naomi Hoevenaars[1], Richard G. Hibbert[1], Andreas Lingnau[1], Ulf Forssmann[1], Janine Schuurman[1], Paul W.H.I. Parren[1,3], Rob N. de Jong[1], and Esther C.W. Breij[1]

ABSTRACT

Higher-order death receptor 5 (DR5) clustering can induce tumor cell death; however, therapeutic compounds targeting DR5 have achieved limited clinical efficacy. We describe HexaBody-DR5/DR5, an equimolar mixture of two DR5-specific IgG1 antibodies with an Fc-domain mutation that augments antibody hexamerization after cell surface target binding. The two antibodies do not compete for binding to DR5 as demonstrated using binding competition studies, and binding to distinct epitopes in the DR5 extracellular domain was confirmed by crystallography. The unique combination of dual epitope targeting and increased IgG hexamerization resulted in potent DR5 agonist activity by inducing efficient DR5 outside-in signaling and caspase-mediated cell death. Preclinical studies *in vitro* and *in vivo* demonstrated that maximal DR5 agonist activity could be achieved independent of Fc gamma receptor–mediated antibody crosslinking. Most optimal agonism was observed in the presence of complement complex C1, although without inducing complement-dependent cytotoxicity. It is hypothesized that C1 may stabilize IgG hexamers that are formed after binding of HexaBody-DR5/DR5 to DR5 on the plasma membrane, thereby strengthening DR5 clustering and subsequent outside-in signaling. We observed potent antitumor activity *in vitro* and *in vivo* in large panels of patient-derived xenograft models representing various solid cancers. The results of our preclinical studies provided the basis for an ongoing clinical trial exploring the activity of HexaBody-DR5/DR5 (GEN1029) in patients with malignant solid tumors.

Introduction

Apoptotic pathways have been identified for targeted therapeutics against multiple disease states, including cancer (1). One such pathway comprises TRAIL that binds to TNF receptor superfamily members death receptor 4 (DR4) and death receptor 5 (DR5), to induce caspase-mediated cell death (2). The discovery that TRAIL-induced, caspase-mediated apoptosis preferentially kills malignant cells informed the potential of this pathway as a target for cancer therapeutics, and led to the development of several mAbs selectively targeting DRs (3). Unfortunately, findings to date showed that most of these compounds failed to provide significant antitumor efficacy in clinical trials.

DR5 aggregation and higher-order clustering at the cell membrane is required for efficient signal transduction, and is an important determinant of response to ligand binding (4, 5). *In vitro* and *in vivo* experiments showed that previously tested DR5 agonist IgG antibodies required secondary antibody crosslinking via Fc gamma receptor (FcγR)-expressing effector cells for optimal DR5 clustering and apoptosis induction (6, 7). The limited success of DR5 antibodies in clinical trials may be the result of insufficient FcγR-mediated crosslinking in the tumor microenvironment (8–10). Alternative mechanisms to induce aggregation and clustering independent of FcγR have also been explored, but limited efficacy data have been published, and in some cases, adverse events and toxicity signals were observed (3, 11, 12). Moreover, preclinical studies have suggested that dual epitope targeting can contribute to enhanced agonistic activity of DR5 antibodies (13).

Through specific noncovalent interactions between IgG Fc domains, IgG antibodies can form ordered antibody hexamers on cell surfaces upon antigen binding (14–16). These ring structures of target-bound antibodies form an optimal docking structure for C1q, the first component of the classical pathway of complement activation (16, 17). The hexavalent C1q molecule, which contains antibody-binding sites, complexes with four proteases (two molecules each of C1r and C1s) to form C1 (18). A single point mutation, such as E430G, in the IgG1 Fc region was shown to enhance ordered hexamer formation through intermolecular Fc–Fc interactions by IgG monomers upon binding to membrane-bound antigens (HexaBody® platform; ref. 14). Moreover, enhanced hexamerization was previously shown to enhance or unlock the capacity of mAbs to induce complement-dependent cytotoxicity (14, 15). We hypothesized that enhanced IgG hexamer formation could also enhance or drive the clustering of plasma membrane receptors, specifically DR5.

In this study, we investigated the application of dual epitope targeting combined with enhanced hexamerization by introducing the E430G hexamerization-enhancing mutation into two noncompeting humanized DR5-targeting antibodies to create

[1]Genmab, Utrecht, the Netherlands, Copenhagen, Denmark, Princeton. [2]iDD biotech, Lyon, France. [3]Department of Immunohematology and Blood Transfusion, Leiden University Medical Center, Leiden, the Netherlands.

Note: Supplementary data for this article are available at Molecular Cancer Therapeutics Online (http://mct.aacrjournals.org/).

M.B. Overdijk and K. Strumane contributed equally to this article.

Current address for T. Kroes: Robinson Research Institute and Adelaide Medical School, University of Adelaide, Adelaide, Australia; and current address for P.W.H.I. Parren, Lava Therapeutics, Utrecht, the Netherlands.

Corresponding Author: Esther C.W. Breij, Genmab, Uppsalalaan 15, 3584CT, Utrecht, The Netherlands; E-mail: ebj@genmab.com

Mol Cancer Ther 2020;19:2126–38

doi: 10.1158/1535-7163.MCT-20-0044

an FcγR-independent DR5 agonist. We also examined the therapeutic potential of antibody hexamer-dependent DR5 clustering *in vitro* on 240 cancer cell lines and *in vivo* in a large panel of solid tumor xenograft models.

Materials and Methods

Cell lines

The cell lines and culture media used in this study are summarized in the Supplementary Methods. COLO 205 cancer cells were harvested by pooling the culture supernatant containing nonadherent cells and trypsinized adherent cells. All other cancer cell lines, except WIL2-S and WIL2-S SF suspension cells, were harvested by trypsinization. For trypsinization, adherent cells were incubated with trypsin-EDTA (Gibco, catalog no. 15400-054) diluted in PBS to a final concentration of 0.05% trypsin for 2 minutes at 37°C and passed through a cell strainer.

Antibodies

DR5 antibodies were obtained by hybridoma technology after immunization of BALB/c mice with soluble recombinant human DR5 protein (R&D Systems. catalog no. 631-T2) and humanization by direct complementarity determining region grafting, backmutations, and optimization. Humanized antibodies were expressed as IgG1m(f). Mutated IgG1 variants with mutation(s) E430G, E430G/K429E, E430G/S440K, L234F/L235E/D265A, L234F/L235E/D265A/E430G, and P329R/E430G were generated by GeneArt Gene Synthesis (Thermo Fisher Scientific) numbered according to Eu nomenclature (19). Antibody Fab fragments were generated by GeneArt Gene Synthesis with a C-terminal His6 tag on the heavy chain and produced using the Expi293F Expression System (Gibco, catalog no. A14635). HexaBody-DR5/DR5 is a 1:1 mixture of the two antibodies Hx-DR5-01 + Hx-DR5-05 (WO2017/093448 SEQ ID no.:38-39 and 42-43). The HIV gp120-specific human antibody IgG1-b12 was used as a nonbinding isotype control antibody (20). Recombinant antibodies were expressed as IgG1κ by transient transfection of Expi293F cells using 293fectin. Antibodies were purified by immobilized protein A chromatography and concentration was measured by absorbance at 280 nm. Quality control of purified antibodies was performed by different methods as described previously (14); Capillary electrophoresis sodium dodecyl sulfate (CE-SDS) on the Labchip GXII (Caliper Life Sciences/PerkinElmer Hopkinton) under reducing and nonreducing conditions (>90% intact IgG, >95% HC + LC under reducing conditions), Electrospray Ionization Time-of-Flight Mass Spectrometry (ESI-TOF MS) (Waters) or Orbitrap (Thermo Fisher Scientific), and High performance size-exclusion chromatography (HP-SEC) (aggregate level < 5%; Waters Alliance 2975 separation unit, Waters). Antibody Fab fragments were purified using immobilized metal affinity chromatography.

Recombinant protein production

Recombinant DR5 extracellular domain (ECD) proteins kDR5ECDdelHis and kDR5ECDdelCtag, based on UniProtKB O14763-2, were produced containing a His-tag (His) or C-tag, respectively. Amino acids 1–19 of DR5 were replaced by a signal peptide derived from the kappa light chain sequence. Codon-optimized DNA fragments encoding the different DR5 proteins, the dimeric FcγR, and biotin ligase BirA constructs were generated at GeneArt. Details on the constructs used are described in the Supplementary Methods. kDR5ECDdelHis and kDR5ECDdelCtag were produced by transient transfection, the dimeric FcγR constructs (21) diFCGR2AH-HisBAP, diFCGR2AR-HisBAP, diFCGR3AF-HisBAP, and diFCGR3AV-HisBAP were cotransfected with BirA and pMix all using the Expi293F Expression System (Gibco, catalog no. A14635) and purified by immobilized metal affinity chromatography.

ELISA

A total of 100 μL coating antibody was added per well of 96-well flat bottom ELISA plates and incubated overnight at 4°C. After washing the plates, nonspecific binding was blocked for 1 hour at room temperature by adding PBS/0.2% BSA. With washings between incubations, plates were sequentially incubated with protein or antibody diluted in PBS supplemented with 0.025% Tween 20 with 0.2% BSA buffer (30 μg/mL final concentration) for 1 hour at room temperature, secondary antibody for 1 hour at room temperature, and streptavidin-labeled polyhorseradish peroxidase (Sanquin, catalog no. M2032) for 20 minutes at room temperature. After washing, 2,2′-azino-bis (3-ethylbenzothiazoline-6-sulfonic acid; ABTS; Roche, catalog no. 11112597001) was added and incubated for approximately 10 minutes at room temperature protected from light. The substrate reaction was stopped by adding an equal volume of 2% oxalic acid. Fluorescence was measured at 405 nm on a BioTek ELx808 Absorbance Microplate Reader. Details on the different ELISA conditions are described in Supplementary Methods.

Flow cytometry

Binding of antibodies to DR5-positive HCT 116 human colorectal cancer cells and DR5-transfected CHO-S cells was analyzed by flow cytometry; assays were performed at 4°C. A total of 100,000 cells per well were seeded in polystyrene 96-well round bottom plates and pelleted by centrifugation. Cells were resuspended in antibody samples (serial dilution range 0–10 μg/mL in 5-fold dilutions for HCT 116; 10 μg/mL final concentration for CHO-S cells) and incubated for 30 minutes at 4°C. Cells were pelleted by centrifugation and washed twice. Cells were incubated with secondary R-phycoerythrin–conjugated goat-anti-human IgG F(ab′)2 [Jackson ImmunoResearch, catalog no. 109-116-098 (1/100) for 30 minutes at 4°C, protected from light]. Cells were washed twice, and antibody binding was analyzed on a FACS-Canto II (BD Biosciences).

The effect of the C1q-binding inhibiting mutations was tested by flow cytometry on the HexaBody-DR5/DR5 mutant variants bound to human DR5 expressed on CHO-S cells. Briefly, 100,000 cells per well were plated in round bottom plates and 20 μg/mL final concentration antibody samples were added. After 15-minute incubation at 37°C, purified human C1q (Quidel, #A400) was added to the cell suspensions as a 3× dilution range between 7.5 μg/mL and 1.1 ng/mL. After an incubation period of 45 minutes at 4°C, cells were washed twice with FACS buffer [PBS + 0.1% (w/v) BSA + 0.02% (w/v) sodium azide] and incubated with FITC-conjugated rabbit anti-human C1q antibody (DAKO, #F0254; 20 μg/mL) for 30 minutes at 4°C, protected from light. Cells were washed twice, resuspended in FACS buffer, and C1q binding to the cells was determined by flow cytometry on an iQue screener (Intellicyt).

Crystallization, data collection, structure determination, and refinement

Complex formation, crystallization, crystallographic data collection, processing, and structure determination were performed by Proteros. Details are described in Supplementary Methods.

Viability assay

Cell viability after antibody treatments was determined using the CellTiter-Glo luminescent cell viability assay (Promega, #G7571,

according to the supplier's protocol). Briefly, 5,000 cells per well were seeded in polystyrene 96-well flat bottom plates and allowed to adhere overnight at 37°C. The following day, antibody samples were added to the adherent cells and incubated for 3 days at 37°C. As a source of C1q, either heat-inactivated Donor Bovine Serum with Iron (Life Technologies, #10371-029) containing sufficient residual intact C1q levels or purified human C1q (2.5 μg/mL final concentration) was added to support maximal potency. PBS or polyclonal anti-human IgG F(ab′)2 fragment (Jackson ImmunoResearch, #109-006-098; 1/150) was added to antibody samples where indicated. For viability assays to assess the cytotoxicity of HexaBody-DR5/DR5 in the presence and absence of a caspase inhibitor, antibody samples were added to the adherent cells followed by pan-caspase inhibitor Z-VAD-FMK (Bachem, #4026865.0005; 5 μmol/L end concentration). As a positive control in all viability assays, cells were incubated with 5 μmol/L staurosporine (Sigma-Aldrich, catalog no. S6942), and untreated cells were included as the negative control. From the kit, 15 μL Luciferin Solution Reagent was added to each well of the viability assay plate. Next, plates were incubated for 1.5 hours at 37°C. Supernatant was transferred to a white OptiPlate-96 and luminescence was measured on an EnVision Multilabel Reader (PerkinElmer). The percentage of viable cells was calculated using the following formula:

$$\%\,\text{viable cells} = \frac{T-P}{V-P} \times 100$$

T = luminescence of the test sample, P = luminescence of staurosporine control sample, and V = luminescence of the medium control sample.

The screening of 240 solid cancer cell lines was performed at Horizon Discovery Ltd. A total of 500 cells per well were seeded in black 384-well assay plates (Corning) and allowed to adhere overnight at 37°C. The following day, antibody samples were added and incubated for 3 days at 37°C (except for DLD-1 and HCT-116 cell lines, for which a 120-hour assay was performed). Viability of the cultured cells was determined in an ATPlite 1step Luminescence Assay System (Perkin Elmer, #6016739), whereby 15 μL ATPlite suspension was added per assay well and luminescence was measured on an ultrasensitive luminescence EnVision Plate Reader (Perkin Elmer). Percentage viability was calculated using the formula:

$$\%\,\text{viable cells} = \frac{T-V(0)}{V-V(0)} \times 100$$

$V(0)$ and V = luminescence of the medium control sample on day 0 and 3, respectively. If $T<V(0)$ then percentage viability = 0%. Tumor types for which more than five cell lines were included in the panel, the percentage of responding cell lines was calculated.

Caspase-3/7 activation

Caspase-3/7 activation following antibody treatments was determined using Caspase-Glo 3/7 assay (Promega, #G8091) according to the supplier's protocol. Briefly, 4,000 cells per well were seeded in 384-well culture plates followed by 16 hours incubation at 37°C. The following day, antibody samples was added and incubated for 1, 2, 4, and 6 hours at 37°C. Plates were removed from the incubator to let the temperature decrease to room temperature. Supernatant was removed before adding Caspase-Glo 3/7 substrate. After mixing by shaking for 1 minute, the plates were incubated for 1 hour at room temperature. Luminescence was measured on an EnVision Multilabel Reader (PerkinElmer).

Mouse tumor xenograft models

The *in vivo* therapeutic activity of HexaBody-DR5/DR5 was tested in cell line– (CDX) and patient-derived (PDX) models at Genmab, Crown Biosciences, Inc or by Champions Oncology as summarized in the Supplementary Methods. All animal experiments were conducted following protocols approved by institutional ethical committees.

CDX tumors were induced by subcutaneous injection of a 100–200 μL tumor cell suspension in the flank of a 7–10 weeks old mouse. For PDX studies, 4–13 weeks old mice were inoculated subcutaneously at the right or rear flank with a tumor fragment of 2-3 mm diameter or 200 μL tumor cell suspension. Tumor volumes were measured at least twice weekly using a digital caliper (Plexx) as follows: Tumor volume (mm^3) = 0.5 × (length) × $(\text{width})^2$.

Mice were divided into groups of 6–8, with equal tumor size distribution (average and variance). For the PDX mouse clinical trials, a one mouse per group design was used. Mice were injected with test solution 0.1 mL/mouse or 10 μL/g bodyweight as specified in the figure legends. Injections were administered intravenously except for the HCT-116 condition for which injections were performed intraperitoneally. Mice were observed at least twice a week for clinical signs of illness. The experiment ended for individual mice when the tumor size exceeded 1.5 cm^3, the tumor showed ulceration, serious clinical illness occurred, when the tumor growth blocked the movement of the mouse, or when tumor growth assessment had been completed. For the PDX mouse clinical trial, the relative tumor growth, between 7 and maximally 25 days after initiation of treatment, was defined as the ratio between the tumor growth in the HexaBody-DR5/DR5-treated mouse (ΔT) and the control mouse (ΔC), specifically ΔT/ΔC. Models in which the control mouse tumor volume did not increase 2-fold after start treatment were excluded from analysis.

Quantification and statistical analysis

Log-transformed data were analyzed and plotted using nonlinear regression [log (inhibitor) vs. response with variable slope] by GraphPad Prism 8 software. Statistical analysis of differences compared with the isotype control in Kaplan–Meier curves representing the percentage mice with a tumor size cut-off of 500 mm^3 was performed by log-rank (Mantel–Cox) analysis using SPSS statistical software (IBM).

Results

Hx-DR5-01 and Hx-DR5-05 bind nonoverlapping DR5 epitopes

Two murine DR5 antibody clones were humanized, cloned in a human IgG1 backbone, and designated IgG1-DR5-01 and IgG1-DR5-05. These antibodies were modified by adding an E430G hexamerization-enhancing mutation in the Fc domain to create Hx-DR5-01 and Hx-DR5-05. Preclinical immunogenicity assessment for Hx-DR5-01 and Hx-DR5-05 *in silico* and *in vitro* indicated low risk of clinical immunogenicity (Supplementary Methods). The two antibodies showed comparable affinity for DR5 in the nanomolar range, which was not affected by the E430G mutation (**Fig. 1A**; Supplementary Table S1). Binding competition studies demonstrated that the two DR5-specific antibodies recognize noncompeting epitopes (**Fig. 1B**). To identify the epitopes for Hx-DR5-01 and Hx-DR5-05, we determined the crystal structure of the ternary complex of the human DR5 ECD in complex with the Fab domains of Hx-DR5-01 and Hx-DR5-05 (DR5-01-Fab and DR5-05-Fab, respectively) at 3.05 Å resolution (**Fig. 1C**; Supplementary Table S2). DR5-01-Fab binds to cysteine-rich domain (CRD)2 and CRD3 of DR5 between residues 115 and 158, while DR5-05-Fab binds to CRD1 and CRD2 between residues 74 and 112. The interaction of DR5-01-Fab with DR5 ECD involves all six

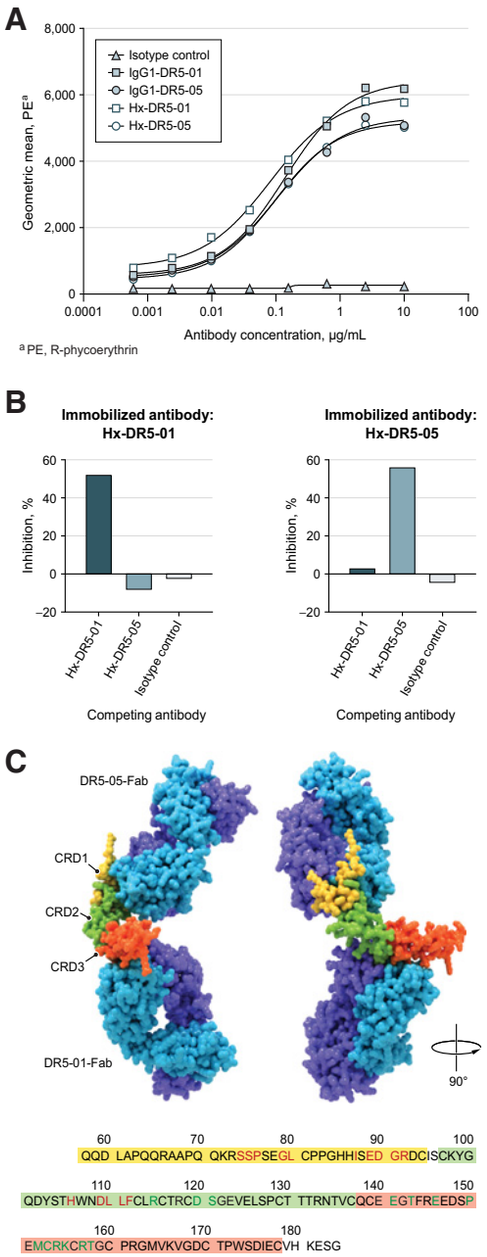

Figure 1.

Binding characteristics of Hx-DR5-01 and Hx-DR5-05. **A,** Binding of Hx-DR5-01 and Hx-DR5-05 to HCT 116 colorectal cancer (CRC) cells was measured by flow cytometry and compared with the wild-type antibodies without the hexamerization-enhancing mutation E430G. The graph shows the geometric mean fluorescence of duplicate measurements of a representative experiment ($n \geq 5$). **B,** Crossblock binding ELISA with immobilized Hx-DR5-01 (left graph) and immobilized Hx-DR5-05 (right graph) in the presence of ECD of DR5 and the indicated competing antibodies. Data show percentage inhibition of binding to DR5 and is the mean of triplicate samples. **C,** Crystal structure of ternary complex of ECD of DR5 bound by Hx-DR5-01 and Hx-DR5-05 Fab fragments shown as a ribbon representation. The heavy chains are shown in blue and the light chains in purple. The CRD1, CRD2, and CRD3 of DR5 are shown in yellow, green, and orange, respectively. The same color coding for the CRD regions is applied for the boxed amino acid sequence; the contact residues for DR5-05-Fab are shown in red and DR5-01-Fab in green. PE, R-phycoerythrin; CRC, colorectal cancer.

complementarity-determining regions and is stabilized by a number of polar contacts including hydrogen bonds to DR5 residues Asp120, Ser121, Glu141, and Glu146. DR5-05-Fab binds predominantly with heavy chain CDR3 and the interaction is stabilized by a salt bridge between Arg98 on DR5-05 heavy chain and Asp109 within DR5 CRD2.

Combining dual epitope targeting and enhanced hexamerization strongly potentiated antitumor activity of DR5 antibodies *in vitro* and *in vivo*

We used Hx-DR5-01 and Hx-DR5-05 to test the hypothesis that cell surface binding of DR5 antibodies with a hexamerization-enhancing mutation, either alone or as a mixture, could promote DR5 agonist activity through higher-order clustering on human tumor cells (**Fig. 2**). First, in the colorectal cancer cell line COLO 205, known to be highly sensitive to DR5 targeting, both Hx-DR5-01 and Hx-DR5-05 induced direct cytotoxicity, whereas their wild-type counterparts did not show any activity (**Fig. 2A**). When equimolar mixtures of the noncompeting wild-type antibodies IgG1-DR5-01 + IgG1-DR5-05 (referred to collectively as IgG1-DR5/DR5) or hexamerization-enhanced antibodies Hx-DR5-01 + Hx-DR5-05 (referred to collectively as HexaBody-DR5/DR5) were administered to COLO 205 cells to test whether dual epitope targeting could contribute to DR5 agonist activity, both mixtures led to a strong increase in cytotoxic activity compared with the individual antibodies. Moreover, HexaBody-DR5/DR5 displayed a significantly lower average IC_{50} (~5-fold) than IgG1-DR5/DR5 (average $IC_{50} \pm$ SD of three independent experiments; 0.008 ± 0.003 μg/mL and 0.041 ± 0.007 μg/mL, respectively; **, $P = 0.005$ paired t test), demonstrating that optimal potency was achieved when dual epitope targeting was combined with enhanced antibody hexamerization. Interestingly, a bispecific antibody carrying one Fab arm from IgG1-DR5-01 and one Fab arm from IgG1-DR5-05 (designated as BisG1-DR5-01-F405L/DR5-05-K409R) was less efficient than the mixture of the parental wild-type antibodies (**Fig. 2A**), suggesting the structural organization of DR5 clusters on the cell surface and resulting cytotoxicity is more efficient when presented as a mixture of two noncompeting antibodies compared with a bispecific antibody.

To further assess the potency of HexaBody-DR5/DR5 in comparison with IgG1-DR5/DR5, we performed additional viability assays using a panel of 12 different human tumor cell lines, including 11 cell lines that are considerably less sensitive to DR5 activation than COLO 205 (22). HexaBody-DR5/DR5 induced dose-dependent cytotoxicity in 11 of the 12 tested cell lines, and in 7 of these 11 responsive cell lines, HexaBody-DR5/DR5 induced significantly higher maximal inhibition of viability compared with IgG1-DR5/DR5 (Supplementary Table S3). A representative result with the colorectal cancer cell line HCT-15 is presented in **Fig. 2**B. Subsequently, using an HCT-15 CDX model, we observed significant antitumor activity *in vivo* by HexaBody-DR5/DR5, and not by the wild-type comparator IgG1-DR5/DR5 or the single hexamerization-enhanced molecules Hx-DR5-01 or Hx-DR5-05 (**Fig. 2C**). DR5 is known to induce cell death in a caspase-dependent manner. To test whether caspase activation is essential for HexaBody-DR5/DR5-induced cell death, we examined the efficacy of HexaBody-DR5/DR5 in BxPC-3 pancreatic cancer cells *in vitro* in the presence of the pan-caspase inhibitor ZVAD, which revealed that cytotoxicity was completely abolished in the presence of the inhibitor (**Fig. 2D**). Consistent with this observation, HexaBody-DR5/DR5-induced potent caspase-3/7 activation (**Fig. 2E**). Both when measuring cell viability and caspase activation, HexaBody-DR5/DR5 was more potent than IgG1-DR5/DR5 (**Fig. 2D** and **E**).

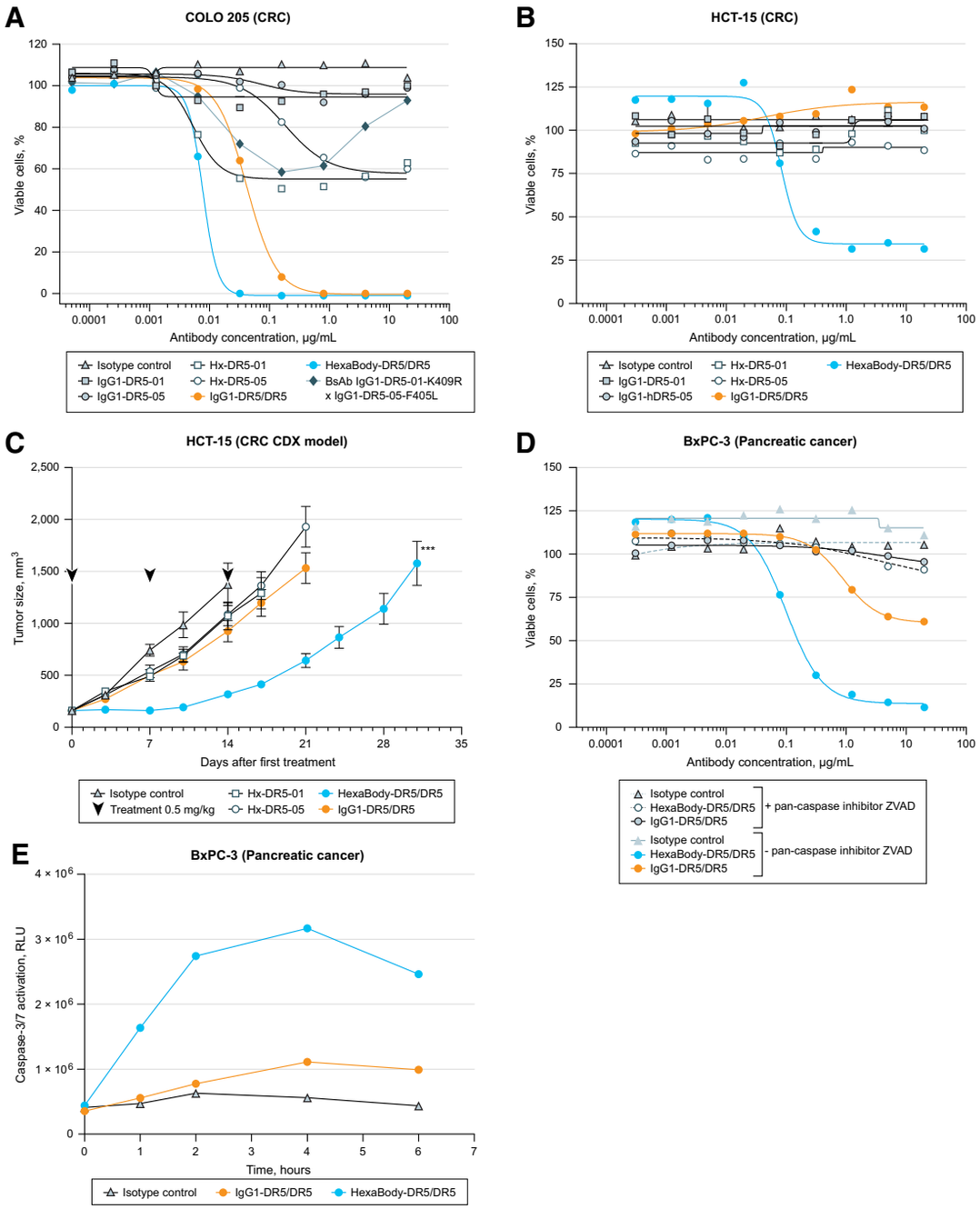

Figure 2.

The HexaBody-DR5/DR5 antibody mixture outperforms the individual hexamerization-enhancing DR5 antibodies and wild-type IgG1 antibodies *in vitro* and *in vivo*, and HexaBody-DR5/DR5 cytotoxicity is caspase dependent. Adherent COLO 205 colorectal cells (**A**), HCT-15 colorectal cells (**B**), and BxPC-3 pancreatic cells (**D**) were incubated with the indicated antibodies with or without 5 µmol/L ZVAD and cell viability was measured after 72 hours. Mean values of duplicate (**D**) or triplicate (**A**/**B**) of a representative experiment ($n \geq 2$) are shown. **C,** A total of 5×10^6 HCT-15 colorectal cancer (CRC) cells were subcutaneously inoculated in BALB/c nude mice and mice were dosed with 0.5 mg/kg of the indicated antibodies ($n = 8$ mice/group). Average tumor size is shown ± SEM. **E,** Adherent BxPC-3 pancreatic cells incubated for 1, 2, 4, or 6 hours in the presence of 1 µg/mL antibody followed by measurement of caspase-3 and -7 activation in a Caspase-Glo 3/7 assay. Mean values of duplicate samples of a representative experiment ($n = 5$) is shown. ***, $P < 0.0001$ [log-rank (Mantel–Cox) test performed on Kaplan–Meier curves for tumor progression]. CRC, colorectal cancer; CDX, cell line–derived xenograft.

We then investigated the relative contributions of Hx-DR5-01 and Hx-DR5-05 by varying the respective concentrations of each molecule in ratios ranging from 1:9 to 9:1. As shown in **Fig. 3** the efficacy of the antibody mixture was independent of the ratio of the single molecules, as long as the limiting antibody concentration was above the IC_{50} for HexaBody-DR5/DR5-induced tumor cell death (see Supplementary Table S3 for cell type–specific IC_{50} values). When the limiting antibody was present at a concentration below IC_{50}, the 1:1 and 1:3 ratios of Hx-DR5-01/Hx-DR5-05 were most potent. On the basis of these results, an equimolar mixture of Hx-DR5-01 and Hx-DR5-05 was selected as a product candidate for clinical development.

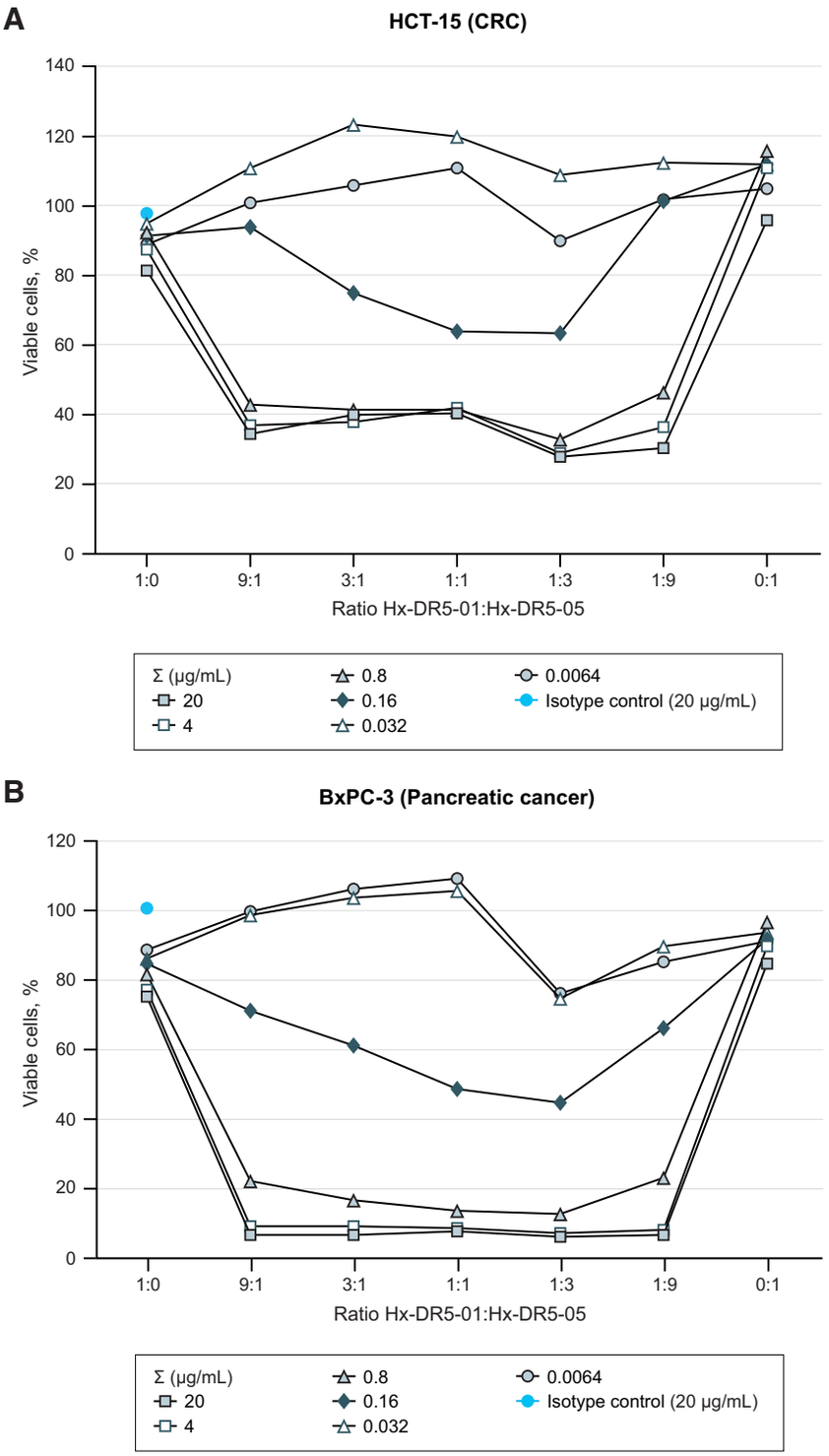

Figure 3.

Effect of different antibody ratios of Hx-DR5-01 and Hx-DR5-05 in HexaBody-DR5/DR5 on cytotoxicity of cancer cells. A 3-day viability assay was performed using HCT-15 colorectal cancer (**A**) and BxPC-3 pancreatic cancer (**B**) cells with the indicated total antibody concentrations (legend) and ratios (*x*-axis) of Hx-DR5-01 and Hx-DR5-05. IgG1-b12 was used as an isotype control antibody. Cell viability was determined using the CellTiter-Glo kit. Mean values of duplicate samples of representative examples [HCT-15 ($n = 2$)] and [BxPC-3 ($n = 3$)] are shown. CRC, colorectal cancer.

Together, these data demonstrate that dual epitope targeting, together with enhanced IgG1 hexamer formation through introduction of the E430G mutation induced highly potent DR5 agonist activity, leading to caspase-dependent apoptosis in cancer cell lines *in vitro* and *in vivo*.

HexaBody-DR5/DR5 cytotoxic activity is dependent on intermolecular Fc–Fc interactions

We further explored the mechanism of HexaBody-DR5/DR5-mediated cytotoxicity by studying the contribution of antibody hexamerization via intermolecular Fc–Fc interactions. First, we used the 13-residue peptide DCAWHLGELVWCT that binds to a hydrophobic patch in the Fc region of antibodies and interferes with IgG Fc–Fc interactions (**Fig. 4A**; refs. 14, 15, 23). In the presence of this peptide, cytotoxic activity of HexaBody-DR5/DR5 in HCT-15 cells was abolished (**Fig. 4B**). Next, Fc–Fc interactions between Hx-DR5-01 or Hx-DR5-05 molecules were modified using mutations K439E and S440K. IgG molecules carrying "self-repelling" mutation K439E or S440K show decreased IgG hexamer formation due to charge repulsion between Fc-domain residues facing each other at the Fc–Fc interface. Charge repulsion can be neutralized by combining antibodies carrying the K439E and S440K mutation, thereby allowing the formation of so-called heterohexamers consisting of antibodies carrying either of the mutations (15, 16, 24; **Fig. 4C**). When Hx-DR5-01 and Hx-DR5-05 carried the same self-repelling mutation, cytotoxic activity of the mixture in BxPC-3 cells was eliminated (**Fig. 4D**). When we used mixtures of Hx-DR5-01-K439E + Hx-DR5-05-S440K or Hx-DR5-01-S440K + Hx-DR5-05-K439E, cytotoxicity in BxPC-3 cells was restored, implicating that heterohexamers are sufficient to drive full potency of HexaBody-DR5/DR5 (**Fig. 4E**).

Together, these results confirm that intermolecular Fc–Fc interactions between the noncompeting DR5-targeting hexamerization-enhanced IgG molecules were essential for DR5 agonist activity by HexaBody-DR5/DR5.

FcγR binding is not required for HexaBody-DR5/DR5 agonist activity in cancer cells

We confirmed that the cytotoxicity of conventional DR5-specific IgG1 mAb conatumumab was completely dependent on the presence of the secondary crosslinker to induce cytotoxicity in a viability assay using BxPC-3 cells and polyclonal anti-human IgG $F(ab')_2$ fragments to mimic FcγR-mediated crosslinking *in vitro* (Supplementary Fig. S1). In contrast, HexaBody-DR5/DR5 showed maximal cytotoxicity both in the presence and absence of the polyclonal anti-human IgG $F(ab')_2$ crosslinker.

To corroborate these *in vitro* findings in an *in vivo* setting, we examined the contribution of FcγR binding to the antitumor activity of conatumumab and HexaBody-DR5/DR5 using a COLO 205 xenograft model. We used FcγR binding–deficient antibody variants by introduction of the L234F/L235E/D265A (FEA) triple mutation. The FEA mutations abrogate interactions with both FcγR and C1 in wild-type IgG1 (25), while C1 binding is preserved and only FcγR binding is abolished by introduction of FEA mutations in antibodies carrying the E430G mutation (Supplementary Figs. S2 and S3). Introduction of these mutations in conatumumab resulted in complete loss of antitumor activity in the COLO 205 xenograft model (**Fig. 5A**). In contrast, no differences in antitumor activity were apparent between HexaBody-DR5/DR5 and its FcγR binding–deficient variant.

That the *in vivo* antitumor activity of HexaBody-DR5/DR5 was maintained in the absence of FcγR binding also suggested that FcγR-mediated effector functions such as antibody-dependent cellular

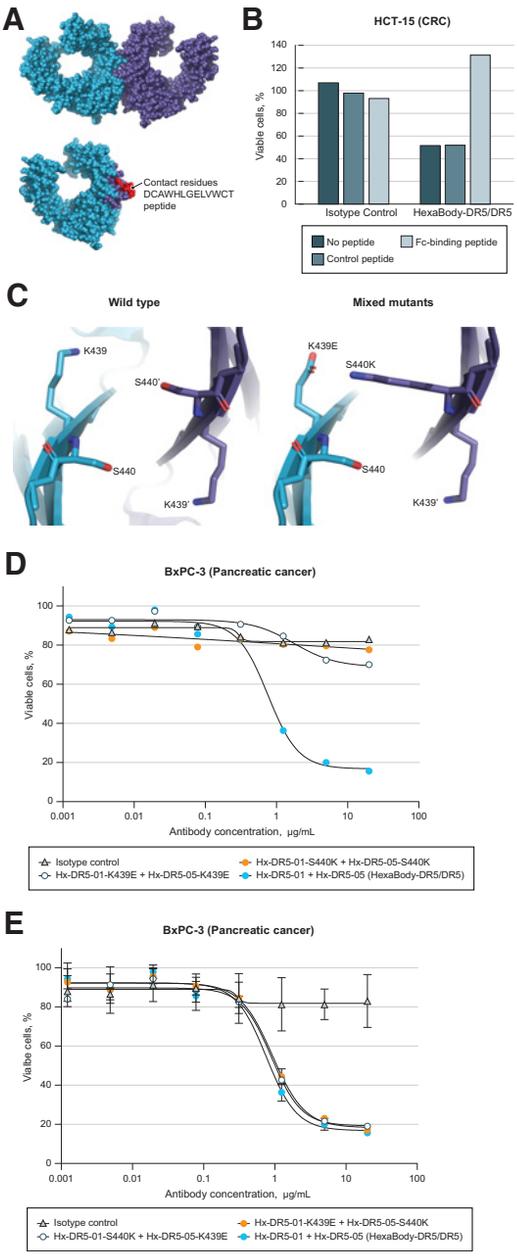

Figure 4.

HexaBody-DR5/DR5 agonist activity is dependent on IgG Fc–Fc interactions and hexamerization. **A,** Previously published biomolecular model of the Fc domain (blue) in contact with the Fc domain of a neighboring antibody (purple) within the IgG1 hexamer, and to the previously published Fc-binding peptide DCAWHLGELVWCT (red) visualized using PyMOL (23). **B,** Adherent HCT-15 CRC cells were incubated with 0.8 μg/mL indicated antibody in absence or presence of 100 μg/mL of the Fc-binding peptide or a scrambled control peptide (WCDLEGVTWHACL). Mean values of quadruplicate samples of a representative experiment ($n = 3$) is shown. **C,** Structural view zoomed to wild-type residues K439 and S440 (left) and the mutations K439E or S440K (right) in both antibodies in the mixture. Antibody variants containing the self-repelling mutations K439E or S440K in either antibody of the mixture (**D**) or both complementary mutations (**E**). After 72 hours, cell viability was measured and mean values of triplicate samples of a representative experiment ($n = 3$) is shown. CRC, colorectal cancer.

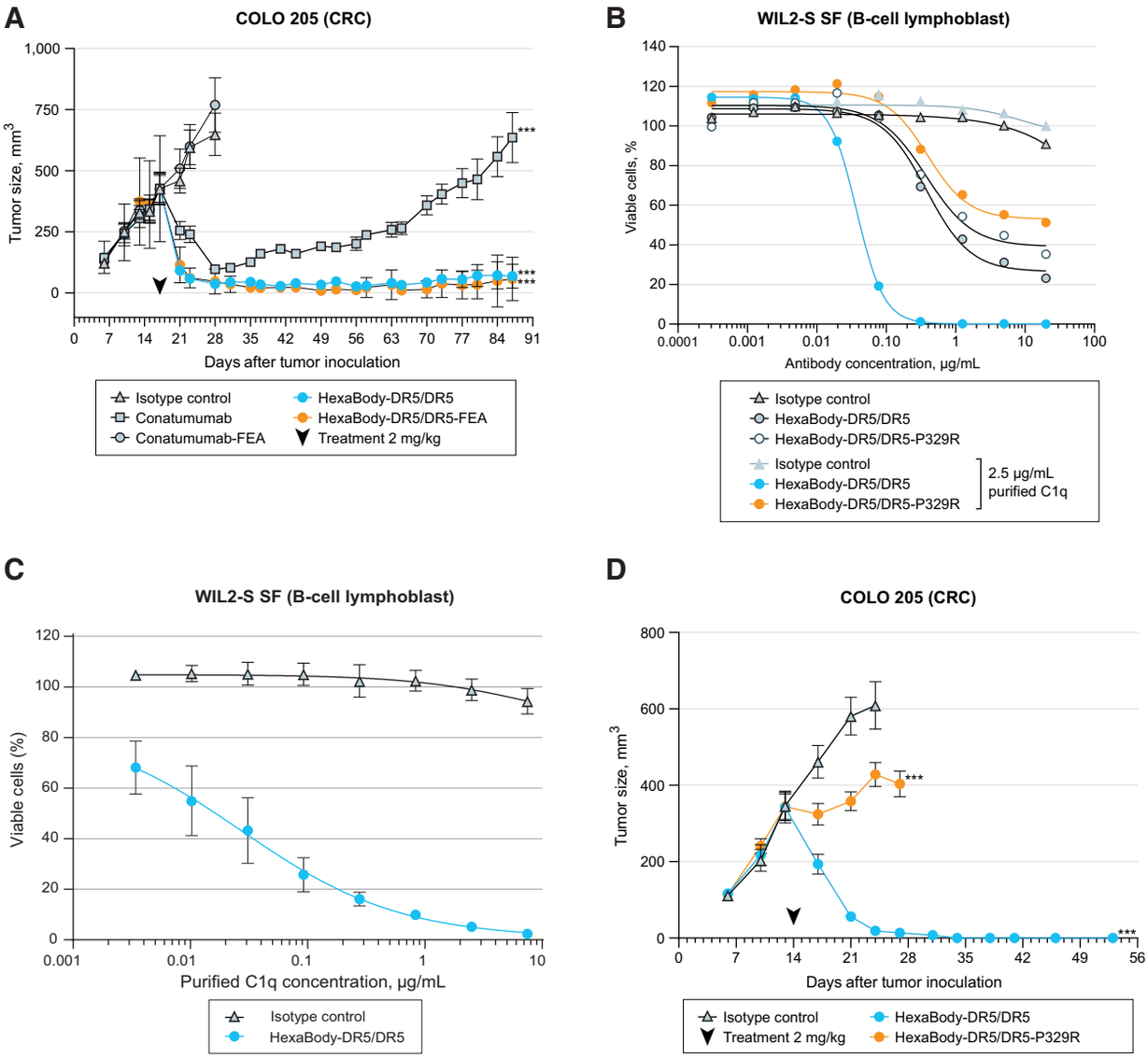

Figure 5.

Cytotoxicity of HexaBody-DR5/DR5 does not depend on FcγR binding and is most optimal in the presence of complement component C1q. **A–D,** A total of 3×10^6 COLO 205 colorectal cancer (CRC) cells were inoculated subcutaneously in CB17-SCID mice and mice were dosed with 2 mg/kg of the indicated antibodies with or without the mutations L234F/L235E/D265A (designated as FEA) or P329R that inhibit C1q and/or FcγR binding ($n = 8$ mice/group). Average tumor size is shown ± SEM. ***, $P < 0.0001$ [log-rank (Mantel–Cox) test performed on Kaplan–Meier curves for tumor progression]. An overnight viability assay was performed with B lymphoblastic WIL2-S SF cells to compare the cytotoxicity of mutant variants in the absence and presence of C1q (**B**) or HexaBody-DR5/DR5 activity (fixed concentration of 0.3 μg/mL) in presence of a serial dilution of C1q (**C**). IgG1-b12 was used as an isotype control antibody. Mean of representative experiments ($n = 3$) are shown. CRC, colorectal cancer.

cytotoxicity (ADCC), did not contribute to the antitumor effect at the tested dose. Therefore, we examined whether HexaBody-DR5/DR5 can stimulate ADCC activity *in vitro* using a chromium release assay with human peripheral blood mononuclear cells (PBMC) as effector cells and HCT 116 CRC cells as target cells. No ADCC activity was observed in four out of five tested donors, while modest activity was observed in presence of PBMCs from the fifth donor (Supplementary Fig. S4).

Taken together, these data demonstrate that antitumor activity of HexaBody-DR5/DR5 does not require FcγR binding *in vitro* or *in vivo*.

Crosslinking by soluble C1 contributes to optimal potency of HexaBody-DR5/DR5 *in vitro* and *in vivo*

The first component of the classical complement pathway is a soluble serum protein complex C1 containing C1q, a hexavalent molecule comprising six Fc-binding globular head pieces, that recognizes surface-bound IgG antibodies organized in hexameric ring structures (15, 17). We hypothesized that the recruitment of C1q to DR5-bound antibodies might stabilize DR5 complexes and promote outside-in signaling. The effect of C1q binding on HexaBody-DR5/DR5 agonist activity was tested using WIL2-S SF cells, a subclone of the

B lymphoblastic cell line WIL2-S adapted to grow in serum-free culture medium, to exclude possible interference from C1 present in culture media serum supplements. WIL2-S SF cells were incubated with HexaBody-DR5/DR5 in the absence or presence of 2.5 μg/mL purified C1q, a concentration well below levels reported in the circulation and tumor microenvironment (26–28). As shown in **Fig. 5B**, the potency and efficacy of HexaBody-DR5/DR5 were most optimal in the presence of C1q (average $IC_{50} \pm$ SD of three independent experiments; 0.37 ± 0.10 μg/mL and 0.04 ± 0.01 μg/mL in absence and presence of C1q, respectively; *, $P = 0.025$ paired *t* test). When C1q was titrated in the presence of a fixed, subsaturating HexaBody-DR5/DR5 concentration, cell death was induced in a C1q dose-dependent fashion with optimal efficacy at ≥2.5 μg/mL purified C1q (**Fig. 5C**). As these experiments were performed in the absence of other complement components, the effect of C1q binding could not be attributed to complement-dependent cytotoxicity (CDC). Moreover, results from dedicated CDC experiments indicated that HexaBody-DR5/DR5 is unable to induce CDC in tumor cells, likely due to low DR5 expression levels (Supplementary Table S4) as CDC was previously shown to require a threshold level of target expression (29, 30). The contribution of complement complex C1 binding to the antitumor activity of HexaBody-DR5/DR5 was further examined *in vivo* using an Fc-inert HexaBody-DR5/DR5 variant carrying mutation P329R that abolishes both FcγR and C1q binding (Supplementary Figs. S2 and S3). While inhibition of FcγR binding alone did not affect *in vivo* efficacy (**Fig. 5A**), additional inhibition of C1 binding significantly reduced antitumor activity compared with HexaBody-DR5/DR5 in the COLO 205 CRC xenograft model (**Fig. 5D**), confirming that C1 binding contributes to optimal activity of HexaBody-DR5/DR5 *in vivo*.

Potent antitumor activity of HexaBody-DR5/DR5 *in vitro* and *in vivo* across tumor types

To support the identification of solid cancers that may respond to HexaBody-DR5/DR5, we investigated the *in vitro* cytotoxicity of HexaBody-DR5/DR5 in viability assays using a large panel of 240 cell lines representing 16 human solid cancer lineages: renal (RCC), lung mesothelioma, colorectal cancer, gastric, pancreatic, liver, endometrial, ovarian, head and neck, urothelial, triple-negative breast cancer (TNBC), non-TNBC, non–small cell lung cancer (NSCLC), small cell lung cancer (SCLC), melanoma, and brain tumors. Cell lines that showed ≤30% tumor cell viability in the presence of HexaBody-DR5/DR5 (i.e., >70% inhibition of tumor cell viability) were classified as

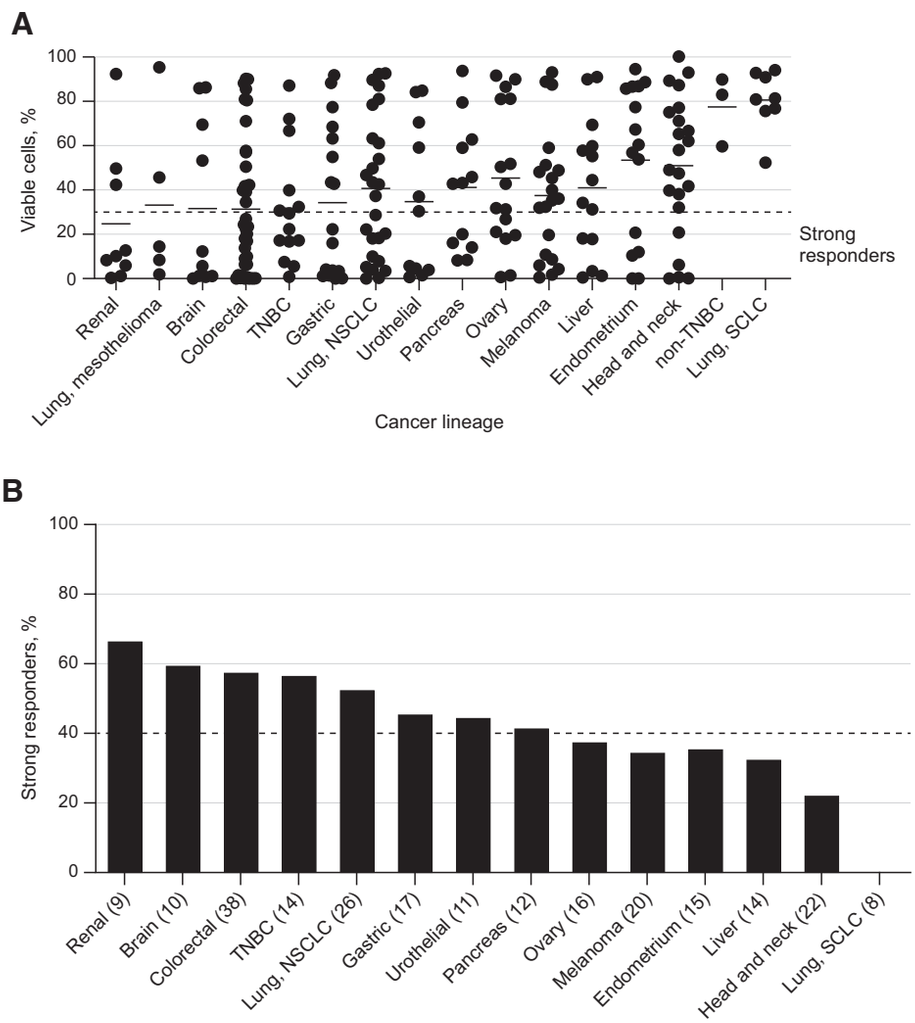

Figure 6.
HexaBody-DR5/DR5 was effective across a broad panel of tumor cell lines. **A,** A 3-day viability assay was performed using a panel of 240 cell lines representing 16 solid cancer lineages. Cell viability was determined using the ATPlite kit. Minimal observed percentage viable cells after incubation with HexaBody-DR5/DR5 is shown, each data point represents an individual cell line of the indicated human cancer type. Cell lines that showed ≤30% viable cells after treatment with HexaBody-DR5/DR5 (indicated by the dotted line) were classified as strong responders. **B,** The percentage of cell lines classified as strong responder within each cancer type/lineage. The total number of cell lines tested is shown in parenthesis. NSCLC, non–small cell lung cancer; SCLC, small cell lung cancer.

Table 1. HexaBody-DR5/DR5 *in vivo* activity in CDX models.

Cell line	Human origin	Dosing schedule	Antitumor activity[a]
HCT-15	CRC	Two doses 0.5, 2, or 10 mg/kg (1QW×2)	Growth inhibition
COLO 205	CRC	Single dose 0.5 or 2 mg/kg	Tumor regression
SW480	CRC	Two doses 0.5, 2, or 10 mg/kg (1QW×2)	Growth inhibition
HCT 116	CRC	Three doses 5 mg/kg (1QW×3)	No effect
BxPC-3	Pancreatic cancer	Two doses 0.5, 2, or 10 mg/kg (1QW×2)	Growth inhibition
PANC-1	Pancreatic cancer	Single dose 10 mg/kg	No effect
A375	Melanoma	Two doses 0.5, 2, or 10 mg/kg (1QW×2)	Growth inhibition
SNU-5	Gastric cancer	Two doses 2 or 10 mg/kg (1QW×2)	Tumor regression
		Two doses 0.5 mg/kg (1QW×2)	Growth inhibition
SK-MES-1	NSCLC	Two doses 0.5, 2, or 10 mg/kg (1QW×2)	Growth inhibition

Note: All doses were administered intravenously except for HCT 116 which was administered intraperitoneally.
Abbreviations: CRC, colorectal cancer; NSCLC, non–small cell lung cancer; QW, once a week.
[a]Antitumor activity (growth inhibition or tumor regression) defined as a statistically significant difference in tumor size between the HexaBody-DR5/DR5 treatment group versus the isotype control IgG1 treatment group [log-rank (Mantel–Cox) test, $P < 0.05$].

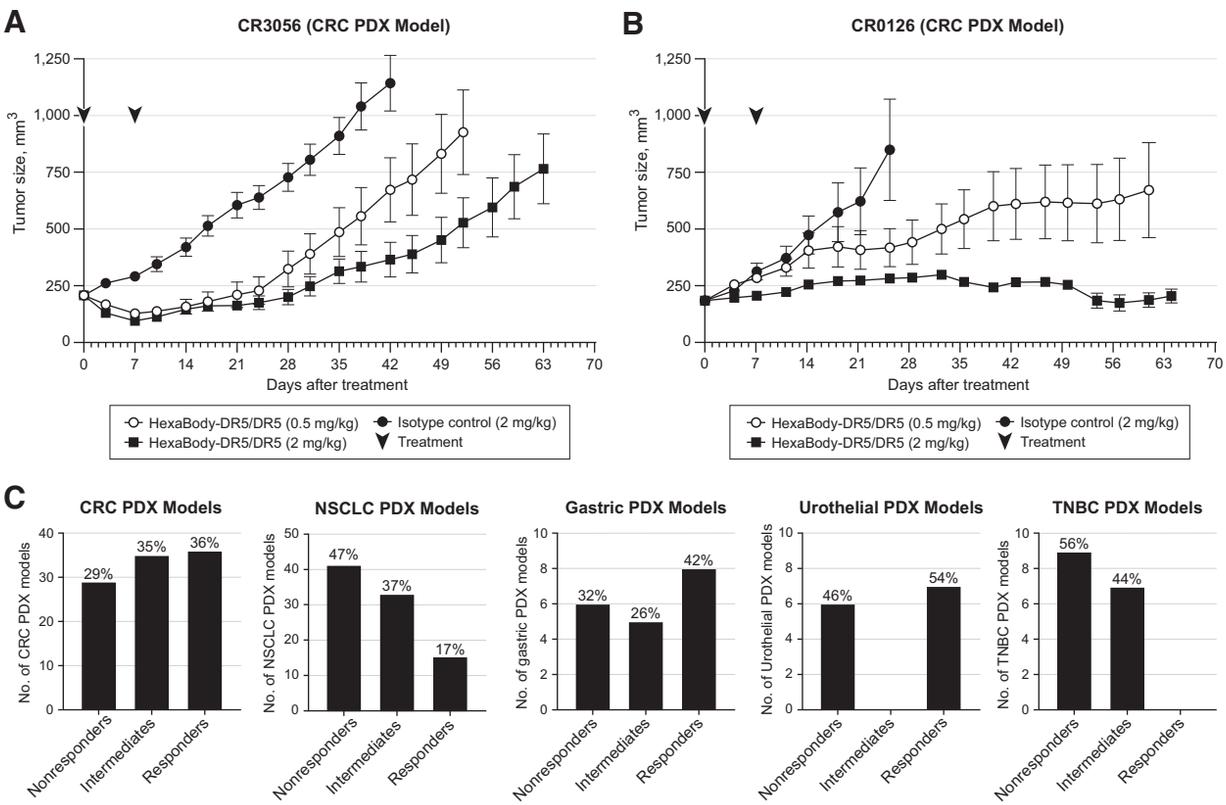

Figure 7.
HexaBody-DR5/DR5 induces potent antitumor activity *in vivo* across tumor types. **A** and **B,** Tumor fragments of PDX models from colorectal cancer (CRC) were SC implanted in Balb/c athymic nude or NU/NU nude mice and mice were dosed with indicated dose of HexaBody-DR5/DR5 or isotype control ($n = 8$ mice/group). Average tumor size is shown ± SEM. **C,** PDX mouse clinical trial performed as described above for regular PDX models from CRC, NSCLC, gastric cancer, urothelial cancer, and TNBC, using a one mouse per group design. Mice were treated with either 2 mg/kg HexaBody-DR5/DR5 or saline buffer. The relative tumor growth was defined as the ratio between the tumor growth in the HexaBody-DR5/DR5 treated mouse (ΔT) and the control mouse (ΔC), specifically ΔT/ΔC. Models were categorized as responders (ΔT/ΔC <10%), intermediates (10% ≤ ΔT/ΔC <70%), or nonresponders (ΔT/ΔC ≥ 70%). CRC, colorectal cancer; NSCLC, non–small cell lung cancer; PDX, patient-derived xenograft; TNBC, triple-negative breast cancer.

strong responders. For all tumor types except non-TNBC and SCLC, at least one responding cell line was identified indicating strong antitumor activity of HexaBody-DR5/DR5 across tumor types (**Fig. 6A**). In RCC, CRC, gastric, urothelial and pancreatic cancer, TNBC, NSCLC, and brain tumors, more than 40% of the tested cell lines showed a strong response to treatment with HexaBody-DR5/DR5 (**Fig. 6B**).

HexaBody-DR5/DR5 also showed therapeutic antitumor activity in seven of nine tested CDX models *in vivo*, including models using colorectal cancer, pancreatic cancer, gastric cancer, NSCLC, and melanoma cell lines (**Table 1**). Statistically significant antitumor activity was observed at the lowest tested dose of 0.5 mg/kg HexaBody-DR5/DR5, and maximal antitumor activity was generally observed at 2 mg/kg with no further enhancement at higher doses. The *in vivo* antitumor activity of HexaBody-DR5/DR5 was confirmed in PDX models for colorectal cancer showing significant antitumor activity (**Fig. 7A** and **B**). In addition, a large screening for HexaBody-DR5/DR5 antitumor activity *in vivo* was performed in a PDX mouse clinical trial using 100 colorectal cancer, 19 gastric, 13 urothelial, 89 NSCLC, and 16 TNBC PDX models, with a one mouse per group design (mice treated with either 2 mg/kg HexaBody-DR5/DR5 or saline control). PDX models were classified as responders when HexaBody-DR5/DR5 induced either tumor stasis or tumor regression ($\Delta T/\Delta C < 10\%$ response). HexaBody-DR5/DR5 showed a substantial proportion of responding PDX models for colorectal cancer [36/100 (36%)], gastric [8/19 (42%)], and urothelial cancer [7/13 (54%); **Fig. 7**C].

Discussion

The discovery of TRAIL and its capacity to selectively induce apoptosis in tumor cells inspired the development of TRAIL-based cancer therapies using two basic strategies: administering recombinant TRAIL (e.g., dulanermin) or agonistic antibodies targeting DRs (e.g., the anti-DR4 antibody mapatumumab, and DR5 mAbs conatumumab, tigatuzumab, drozitumab, lexatumumab, LBY-135, and DS-8273a; refs. 4, 31–40). Although clinical trials demonstrated these approaches were generally safe and well tolerated, they failed to provide significant clinical antitumor efficacy (4, 33, 38, 39). In this study, we investigated a DR5 agonist with a unique mechanism of action compared with previously described DR5 antibodies. We demonstrated the preclinical application of the HexaBody platform to induce tumor cell death through antibody-mediated higher-order DR5 clustering and subsequent outside-in signaling. HexaBody-DR5/DR5 confers dual epitope targeting by the mixture of two noncompeting DR5 mAbs, each carrying the E430G mutation to enhance antibody hexamerization upon binding to DR5 on the cell surface. HexaBody-DR5/DR5 resulted in superior antitumor activity *in vitro* and *in vivo* compared with single DR5 HexaBody molecules or the mixture of wild-type DR5 antibodies across a wide range of tumor types.

The clinical failure of monoclonal DR5 antibodies to show notable antitumor efficacy has been attributed to their dependence on FcγR crosslinking to achieve DR5 clustering and cytotoxic effects (8, 9). In this study, we demonstrated that cytotoxicity of HexaBody-DR5/DR5 did not require FcγR-mediated crosslinking *in vitro* and *in vivo*. These results suggest that HexaBody-DR5/DR5 may be effective in a tumor microenvironment where FcγR-expressing cells may be absent or in short supply. Interestingly, our results demonstrate that the cytotoxic mechanism of HexaBody-DR5/DR5 is independent of complement activation; yet, the presence of complement complex C1 was required for optimal activity, suggesting that C1 can also act as a structural component in the formation or stabilization of antigen complex structures by recognition of antigen-bound antibodies. The concentration of purified C1q required for optimal activity of HexaBody-DR5/DR5 *in vitro* was well below levels reported in the circulation and tumor microenvironment (26–28), and C1 levels are therefore not expected to be limiting in patients.

Several other FcγR-independent DR5 agonists were previously developed for the treatment of cancer (10). The bispecific FAPxDR5 antibody RG7386, aimed to induce DR5 clustering on tumor cells by simultaneous binding of fibroblast-activating protein on cancer-associated fibroblasts and DR5 on cancer cells, was discontinued in 2018 (11, 41). The llama-derived tetravalent DR5 Nanobody TAS266 promoted strong FcγR-independent DR5 clustering in nonclinical studies (42), but liver toxicity possibly related to preexisting anti-nanobody antibodies halted clinical development (12, 43). The DR5 agonist INBRX-109, comprising four humanized DR5 single domain antibody sequences to cluster four DR5 receptors per molecule, is currently in a phase I clinical trial for patients with locally advanced or metastatic solid tumors. Besides DR5-targeting antibodies, TRAIL-derived compounds have also been pursued to mimic target clustering by the natural ligand. ABBV-621, an Fc fusion with six TRAIL receptor binding domains (9, 44, 45), and the covalently trimerized TRAIL fusion protein SCB-313 (46) are currently under investigation in phase I clinical trials. HexaBody-DR5/DR5 is unique from these other compounds by its configuration as monomeric antibodies with a regular IgG1 structure, designed to maintain typical IgG1 pharmacokinetics and biopharmaceutical characteristics (14), and manufacturability. The minimal engineering required for HexaBody-DR5/DR5 (a single point mutation in the human IgG1 Fc backbone) is expected to lower the risk of the immunogenicity-related toxicity in human studies observed with other DR5-targeting antibody formats.

HexaBody-DR5/DR5 induced potent cytotoxicity in 104 tumor cell lines representing many solid cancer lineages, and showed significant antitumor activity in seven of the nine tested CDX models, derived from colorectal cancer, pancreatic cancer, gastric cancer, NSCLC, and melanoma cell lines. *In vivo* efficacy of HexaBody-DR5/DR5 was confirmed in two of three colorectal cancer PDX models, and high response rates were observed in the PDX mouse clinical trials using a large number of patient-derived tumor cells of colorectal cancer, NSCLC, gastric, and urothelial cancer. Despite the fact that combining dual epitope targeting and enhanced antibody hexamerization resulted in strong antitumor activity of HexaBody-DR5/DR5 across many tumor models, resistance to HexaBody-DR5/DR5 was observed for a fraction of tested cell lines and xenograft models. Intrinsic or acquired drug resistance to DR5 antibodies is a known phenomenon, termed "fractional survival," whereby a portion of cells die while others thrive (47, 48). Intrinsic or acquired resistance also contributed to the lack of clinical efficacy of DR-activating compounds in human studies, and companion diagnostics may help predict therapeutic efficacy. Possible mechanisms of resistance to HexaBody-DR5/DR5 are currently being explored.

In conclusion, HexaBody-DR5/DR5 is a mixture of two minimally engineered DR5-targeting IgG1 molecules that induces potent DR5 clustering, outside-in signaling, caspase activation, and target cell death. Three key characteristics of the mechanism of action underlie the effectiveness of HexaBody-DR5/DR5: (i) dual epitope targeting by the mixture of the two antibodies that bind to distinct epitopes on DR5, (ii) enhanced antibody hexamer formation after cell surface target binding due to the Fc–Fc interaction-enhancing mutation, and (3)

recruitment of C1 to hexameric antibody–antigen complexes on the cell surface. Together, the combination of these properties lead to potent DR5 activation and cell death induction. Of note, maximal effect could be achieved in a CDC- and FcγR-independent manner. In our experiments, HexaBody-DR5/DR5 demonstrated potent DR5 agonist activity across a range of preclinical models, including large panels of cell lines and PDX models. A phase I/IIa clinical trial to assess clinical safety of HexaBody-DR5/DR5 (GEN1029) in patients with malignant solid tumors and to determine the MTD and recommended phase 2 dose is currently ongoing (NCT03576131).

Disclosure of Potential Conflicts of Interest

M.B. Overdijk reports other from Dutch government (WBSO; financial support for Research and Development from Dutch government) during the conduct of the study; in addition, M.B. Overdijk has a patent for WO2017093448 pending, a patent for WO2017093447 pending, and a patent for WO2018083126 pending; and Employment and stock or other ownership in Genmab. K. Strumane reports other from Dutch government (WBSO; financial support for Research and Development from Dutch government) during the conduct of the study; in addition, K. Strumane has a patent for WO2017093448 pending, a patent for WO2017093447 pending, and a patent for WO2018083126 pending. F.J. Beurskens reports other from Dutch goverment (WBSO; financial support for Research and Development from Dutch government) during the conduct of the study; in addition, F.J. Beurskens has a patent for WO2013004842 pending, a patent for WO2014108198 pending, a patent for WO2017093447 pending, and a patent for WO2018083126 pending. A. Ortiz Buijsse reports other from Dutch government(WBSO; financial support for Research and Development from Dutch government) during the conduct of the study. C. Vermot-Desroches reports other from iDD biotech (R&D program out licensed to Genmab) during the conduct of the study; other from iDD biotech (R&D program outlicensed to Genmab) outside the submitted work; in addition, C. Vermot-Desroches has a patent for WO2014009358A1 licensed to Genmab. T. Kroes reports other from Dutch government (WBSO; financial support for Research and Development from Dutch government) during the conduct of the study. B. de Jong reports other from Dutch government (WBSO; financial support for Research and Development from Dutch government) during the conduct of the study. N. Hoevenaars reports other from Dutch government (WBSO; financial support for Research and Development from Dutch government) during the conduct of the study. R.G. Hibbert reports other from Dutch government (WBSO; financial support for Research and Development from Dutch government) during the conduct of the study. U. Forssmann reports other from Dutch Government (WBSO; financial support for Research and Development from Dutch government) during the conduct of the study. J. Schuurman reports other from Dutch government (WBSO; financial support for Research and Development from Dutch government) during the conduct of the study; in addition, J. Schuurman has a patent for WO2017093448 pending, a patent for WO2013004842 issued, a patent for WO2014108198 pending, a patent for WO2017093447 pending, and a patent for WO2018083126 pending. P.W.H.I. Parren reports other from Dutch government (WBSO; financial support for Research and Development from Netherlands government) during the conduct of the study; other from Genmab (owns stock) outside the submitted work; in addition, P.W.H.I. Parren has a patent for WO2017093448 pending (assigned to Genmab), a patent for WO2013004842 pending (assigned to Genmab), a patent for WO2014108198 pending (assigned to Genmab), a patent for WO2017093447 pending (assigned to Genmab), and a patent for WO2018083126 pending (assigned to Genmab). R.N. de Jong reports other from WBSO (financial support for Research and Development from Dutch government) during the conduct of the study; in addition, R.N. de Jong has a patent for WO2013004842 issued, a patent for WO2014108198 pending, a patent for WO2017093447 pending, and a patent for WO2018083126 pending. E.C.W. Breij reports other from Dutch Government (WBS0; governmental support research and development) during the conduct of the study; in addition, E.C.W. Breij has a patent for WO2017093448 pending.

Authors' Contributions

M.B. Overdijk: Conceptualization, formal analysis, validation, investigation, methodology, writing-original draft, writing-review and editing. **K. Strumane:** Conceptualization, validation, writing-original draft, writing-review and editing. **F.J. Beurskens:** Conceptualization, writing-review and editing. **A. Ortiz Buijsse:** Investigation, writing-review and editing. **C. Vermot-Desroches:** Conceptualization, writing-review and editing. **B.S. Vuillermoz:** Investigation, writing-review and editing. **T. Kroes:** Investigation, writing-review and editing. **B. de Jong:** Investigation, writing-review and editing. **N. Hoevenaars:** Investigation, writing-review and editing. **R.G. Hibbert:** Formal analysis, methodology, writing-review and editing. **A. Lingnau:** Formal analysis, methodology, writing-review and editing. **U. Forssmann:** Conceptualization, writing-review and editing. **J. Schuurman:** Conceptualization, writing-review and editing. **P.W.H.I. Parren:** Conceptualization, supervision, writing-review and editing. **R.N. de Jong:** Conceptualization, writing-review and editing. **E.C.W. Breij:** Conceptualization, supervision, validation, writing-original draft, writing-review and editing.

Acknowledgments

The authors express their thanks to Marcel Brandhorst and Chantal de Bije for technical assistance and Xiaoguang Xue for providing sequence alignments.

The costs of publication of this article were defrayed in part by the payment of page charges. This article must therefore be hereby marked *advertisement* in accordance with 18 U.S.C. Section 1734 solely to indicate this fact.

Received January 17, 2020; revised June 5, 2020; accepted August 5, 2020; published first August 26, 2020.

References

1. Dove A. Making a living out of the art of dying. Nat Biotechnol 2001;19:615–9.
2. Sessler T, Healy S, Samali A, Szegezdi E. Structural determinants of DISC function: new insights into death receptor-mediated apoptosis signalling. Pharmacol Ther 2013;140:186–99.
3. Kretz A-L, Trauzold A, Hillenbrand A, Knippschild U, Henne-Bruns D, von Karstedt S, et al. TRAILblazing strategies for cancer treatment. Cancers 2019;11:456.
4. Ashkenazi A. Targeting the extrinsic apoptotic pathway in cancer: lessons learned and future directions. J Clin Invest 2015;125:487–9.
5. Pan L, Fu TM, Zhao W, Zhao L, Chen W, Qiu C, et al. Higher-order clustering of the transmembrane anchor of DR5 drives signaling. Cell 2019;176:1477–89.e14.
6. Kaplan-Lefko PJ, Graves JD, Zoog SJ, Pan Y, Wall J, Branstetter DG, et al. Conatumumab, a fully human agonist antibody to death receptor 5, induces apoptosis via caspase activation in multiple tumor types. Cancer Biol Ther 2010;9:618–31.
7. Wilson NS, Yang B, Yang A, Loeser S, Marsters S, Lawrence D, et al. An Fc gamma receptor-dependent mechanism drives antibody-mediated target-receptor signaling in cancer cells. Cancer Cell 2011;19:101–13.
8. de Miguel D, Lemke J, Anel A, Walczak H, Martinez-Lostao L. Onto better TRAILs for cancer treatment. Cell Death Differ 2016;23:733–47.
9. Gieffers C, Kluge M, Merz C, Sykora J, Thiemann M, Schaal R, et al. APG350 induces superior clustering of TRAIL receptors and shows therapeutic antitumor efficacy independent of cross-linking via Fc gamma receptors. Mol Cancer Ther 2013;12:2735–47.
10. Wajant H. Molecular mode of action of TRAIL receptor agonists-common principles and their translational exploitation. Cancers 2019;11:954.
11. Bendell J, Blay J-Y, Cassier P, Bauer T, Terret C, Mueller C, et al. Phase 1 trial of RO6874813, a novel bispecific FAP-DR5 antibody, in patients with solid tumors [abstract]. In: Proceedings of the AACR-NCI-EORTC International Conference: Molecular Targets and Cancer Therapeutics; 2017 Oct 26–30; Philadelphia, PA. Philadelphia (PA): AACR; Mol Cancer Ther 2018;17(1 Suppl):Abstract nr A092.
12. Papadopoulos KP, Isaacs R, Bilic S, Kentsch K, Huet HA, Hofmann M, et al. Unexpected hepatotoxicity in a phase I study of TAS266, a novel tetravalent agonistic Nanobody(R) targeting the DR5 receptor. Cancer Chemother Pharmacol 2015;75:887–95.
13. Yang Y, Yeh SH, Madireddi S, Matochko WL, Gu C, Sanchez PP, et al. Tetravalent biepitopic targeting enables intrinsic antibody agonism of tumor necrosis factor receptor superfamily members. MAbs 2019;11:996–1011.
14. de Jong RN, Beurskens FJ, Verploegen S, Strumane K, van Kampen MD, Voorhorst M, et al. A novel platform for the potentiation of therapeutic

antibodies based on antigen-dependent formation of IgG hexamers at the cell surface. PLoS Biol 2016;14:e1002344.
15. Diebolder CA, Beurskens FJ, de Jong RN, Koning RI, Strumane K, Lindorfer MA, et al. Complement is activated by IgG hexamers assembled at the cell surface. Science 2014;343:1260–3.
16. Strasser J, de Jong RN, Beurskens FJ, Wang G, Heck AJR, Schuurman J, et al. Unraveling the macromolecular pathways of IgG oligomerization and complement activation on antigenic surfaces. Nano Lett 2019;19:4787–96.
17. Ugurlar D, Howes SC, de Kreuk B-J, Koning RI, de Jong RN, Beurskens FJ, et al. Structures of C1-IgG1 provide insights into how danger pattern recognition activates complement. Science 2018;359:794–7.
18. Arlaud GJ, Gaboriaud C, Thielens NM, Rossi V, Bersch B, Hernandez JF, et al. Structural biology of C1: dissection of a complex molecular machinery. Immunol Rev 2001;180:136–45.
19. Kabat EA, Te Wu T, Perry HM, Foeller C, Gottesman KS. Sequences of proteins of immunological interest. Diane Publishing Co. Darby, US. 1992.
20. Barbas CF, Collet TA, Amberg W, Roben P, Binley JM, Hoekstra D, et al. Molecular profile of an antibody response to HIV-1 as probed by combinatorial libraries. J Mol Biol 1993;230:812–23.
21. Wines BD, Vanderven HA, Esparon SE, Kristensen AB, Kent SJ, Hogarth PM. Dimeric Fc gammaR ectodomains as probes of the Fc receptor function of anti-influenza virus IgG. J Immunol 2016;197:1507–16.
22. Reddy A, Growney JD, Wilson NS, Emery CM, Johnson JA, Ward R, et al. Gene expression ratios lead to accurate and translatable predictors of DR5 agonism across multiple tumor lineages. PLoS One 2015;10:e0138486.
23. DeLano WL, Ultsch MH, de Vos AM, Wells JA. Convergent solutions to binding at a protein-protein interface. Science 2000;287:1279–83.
24. Oostindie SC, van der Horst HJ, Lindorfer MA, Cook EM, Tupitza JC, Zent CS, et al. CD20 and CD37 antibodies synergize to activate complement by Fc-mediated clustering. Haematologica 2019;104:1841–52.
25. Engelberts PJ, Hiemstra IH, de Jong B, Schuurhuis DH, Meesters J, Beltran Hernandez I, et al. DuoBody-CD3xCD20 induces potent T-cell-mediated killing of malignant B cells in preclinical models and provides opportunities for subcutaneous dosing. EBioMedicine 2020;52:102625.
26. Bouwens TA, Trouw LA, Veerhuis R, Dirven CM, Lamfers ML, Al-Khawaja H. Complement activation in Glioblastoma multiforme pathophysiology: evidence from serum levels and presence of complement activation products in tumor tissue. J Neuroimmunol 2015;278:271–6.
27. Bulla R, Tripodo C, Rami D, Ling GS, Agostinis C, Guarnotta C, et al. C1q acts in the tumour microenvironment as a cancer-promoting factor independently of complement activation. Nat Commun 2016;7:10346.
28. Grevys A, Bern M, Foss S, Bratlie DB, Moen A, Gunnarsen KS, et al. Fc engineering of human IgG1 for altered binding to the neonatal Fc receptor affects Fc effector functions. J Immunol 2015;194:5497–508.
29. van Meerten T, van Rijn RS, Hol S, Hagenbeek A, Ebeling SB. Complement-induced cell death by rituximab depends on CD20 expression level and acts complementary to antibody-dependent cellular cytotoxicity. Clin Cancer Res 2006;12:4027–35.
30. Loeff FC, van Egmond HME, Nijmeijer BA, Falkenburg JHF, Halkes CJ, Jedema I. Complement-dependent cytotoxicity induced by therapeutic antibodies in B-cell acute lymphoblastic leukemia is dictated by target antigen expression levels and augmented by loss of membrane-bound complement inhibitors. Leuk Lymphoma 2017;58:1–14.
31. Dimberg LY, Anderson CK, Camidge R, Behbakht K, Thorburn A, Ford HL. On the TRAIL to successful cancer therapy? Predicting and counteracting resistance against TRAIL-based therapeutics. Oncogene 2013;32:1341–50.
32. Lemke J, von Karstedt S, Zinngrebe J, Walczak H. Getting TRAIL back on track for cancer therapy. Cell Death Differ 2014;21:1350–64.
33. von Karstedt S, Montinaro A, Walczak H. Exploring the TRAILs less travelled: TRAIL in cancer biology and therapy. Nat Rev Cancer 2017;17:352–66.
34. Hotte SJ, Hirte HW, Chen EX, Siu LL, Le LH, Corey A, et al. A phase 1 study of mapatumumab (fully human monoclonal antibody to TRAIL-R1) in patients with advanced solid malignancies. Clin Cancer Res 2008;14:3450–5.
35. Vulfovich M, Saba N. Technology evaluation: mapatumumab, Human Genome Sciences/GlaxoSmithKline/Takeda. Curr Opin Mol Ther 2005;7:502–10.
36. Forero A, Bendell JC, Kumar P, Janisch L, Rosen M, Wang Q, et al. First-in-human study of the antibody DR5 agonist DS-8273a in patients with advanced solid tumors. Invest New Drugs 2017;35:298–306.
37. Dominguez GA, Condamine T, Mony S, Hashimoto A, Wang F, Liu Q, et al. Selective targeting of myeloid-derived suppressor cells in cancer patients using DS-8273a, an agonistic TRAIL-R2 antibody. Clin Cancer Res 2017;23:2942–50.
38. Holland PM. Death receptor agonist therapies for cancer, which is the right TRAIL? Cytokine Growth Factor Rev 2014;25:185–93.
39. Amarante-Mendes GP, Griffith TS. Therapeutic applications of TRAIL receptor agonists in cancer and beyond. Pharmacol Ther 2015;155:117–31.
40. Wiezorek J, Holland P, Graves J. Death receptor agonists as a targeted therapy for cancer. Clin Cancer Res 2010;16:1701–8.
41. Brünker P, Wartha K, Friess T, Grau-Richards S, Waldhauer I, Koller CF, et al. RG7386, a novel tetravalent FAP-DR5 antibody, effectively triggers FAP-dependent, avidity-driven DR5 hyperclustering and tumor cell apoptosis. Mol Cancer Ther 2016;15:946–57.
42. Huet HA, Growney JD, Johnson JA, Li J, Bilic S, Ostrom L, et al. Multivalent nanobodies targeting death receptor 5 elicit superior tumor cell killing through efficient caspase induction. MAbs 2014;6:1560–70.
43. Iezzi ME, Policastro L, Werbajh S, Podhajcer O, Canziani GA. Single-domain antibodies and the promise of modular targeting in cancer imaging and treatment. Front Immunol 2018;9:273.
44. Fleten KG, Flørenes VA, Prasmickaite L, Hill O, Sykora J, Mælandsmo GM, et al. hvTRA, a novel TRAIL receptor agonist, induces apoptosis and sustained growth retardation in melanoma. Cell Death Discov 2016;2:16081.
45. Ratain MJ, Doi T, De Jonge MJ, LoRusso P, Dunbar M, Chiney M, et al. Phase 1, first-in-human study of TRAIL receptor agonist fusion protein ABBV-621. J Clin Oncol 2019;37:15s, (suppl; abstr 3013).
46. Liu H, Su D, Zhang J, Ge S, Li Y, Wang F, et al. Improvement of pharmacokinetic profile of TRAIL via trimer-tag enhances its antitumor activity *in vivo*. Sci Rep 2017;7:8953.
47. Flusberg DA, Roux J, Spencer SL, Sorger PK. Cells surviving fractional killing by TRAIL exhibit transient but sustainable resistance and inflammatory phenotypes. Mol Biol Cell 2013;24:2186–200.
48. Shlyakhtina Y, Pavet V, Gronemeyer H. Dual role of DR5 in death and survival signaling leads to TRAIL resistance in cancer cells. Cell Death Dis 2017;8:e3025.